Heating of the spin system by nonequilibrium phonons in semimagnetic (Cd,Mn,Mg)Te quantum wells

A. V. Scherbakov and A. V. Akimov
A. F. Ioffe Physical-Technical Institute, Russian Academy of Sciences, 194021 St. Petersburg, Russia

D. R. Yakovlev,* W. Ossau, A. Waag, and G. Landwehr
Physikalisches Institut der Universität Würzburg, 97074 Würzburg, Germany

T. Wojtowicz, G. Karczewski, and J. Kossut
Institute of Physics, Polish Academy of Sciences, 02-668 Warsaw, Poland
(Received 10 February 1999; revised manuscript received 28 April 1999)

We study the heating of the spin system of magnetic ions induced by ballistic acoustic nonequilibrium phonons in (Cd,Mn,Mg)Te-based semimagnetic quantum wells using exciton luminescence technique. We find that the temperature of the spin system in the presence of nonequilibrium phonons decreases with the increase of magnetic field. In the analysis, we use the well-known fact that phonon losses at the solid/liquid helium boundary increase with the increase of phonon energy. The results lead us to the conclusion that the spin-heating effect is induced by phonons with energies resonant to the Zeeman splitting of spin sublevels of Mn ions. We propose a type of the subterahertz phonon spectrometer that may be used for investigation of semiconductor nanostructures. [S0163-1829(99)04831-6]

I. INTRODUCTION

Experiments with nonequilibrium acoustic terahertz and subterahertz phonons provide important information about vibrational and electron properties of solids.[1,2] In *semiconductor nanostructures* the nonequilibrium phonon technique has been successfully used during last decade in order to study the interaction of acoustic phonons with carriers and excitons in quantum wells and two-dimensional heterostructures.[3,4] The wavelength of acoustic high-energy ($\hbar\omega \sim 1$ meV) phonons ($\lambda \sim 10$ nm) is in the order of the size of semiconductor nanolayers and nanoparticles. Thus, one expects, that experiments with high-energy phonons in the samples with semiconductor nanostructures would be very useful for understanding of the quantum confinement effects and their influence on the properties of carriers, phonons, and electron-phonon interaction.

The most fruitful information may be obtained using phonon spectroscopy techniques that use high-energy phonon generators and detectors with narrow phonon energy band. Only a few high-resolution phonon spectroscopy experiments have been carried out in semiconductor nanostructures. Almost all of them use superconducting tunnel junction devices for generation and detection of phonons.[5] Narayanamurti *et al.*[6] used this technique studying the phonon transmission in GaAs/(Al,Ga)As superlattices and observed the stopbands in the phonon dispersion. Later Tamura, Hurley, and Wolfe[7] studied properties of phonons in GaAs/AlAs superlattices in more details. Hensel and Dynes[8] used superconducting tunnel junctions to study the absorption of phonons by two-dimensional electron gas and Rothenfusser, Kösfer, and Dietsche[9] used the similar technique to study the phonon emission from Si metal-oxide semiconductor field-effect transistor. Superconducting tunnel junction experiments in subterahertz region require low temperatures ($T < 1$ K), zero-magnetic field, and extremely low power of generated phonons, which limit the application of this technique in phonon spectroscopy experiments with semiconductor nanostructures. Actually, using the superconducting tunnel junctions it is possible to detect the nonequilibrium phonons that are transmitted through or reflected from the semiconductor nanostructure. However, it would be very useful to study phonon dynamics with spectral resolution just *inside* the semiconductor nanostructure similar to the way how it is done using the exciton luminescence in GaAs epilayers[10] and quantum wells.[11] The work on the development of phonon spectroscopy techniques is carried out actively nowadays. Recently Oualt *et al.*[12] proposed to use semiconductor tunneling device (double barrier tunneling diodes and superlattices) as a phonon detector with moderate spectral resolution. Cooper *et al.*[13] are working on creating a phonon spectrometer based on the tunneling from a normal metal state.

In the present paper, we propose a technique that may be used as a high-resolution phonon spectrometer in 0.1–1 meV (25–250 GHz) range in semiconductor nanostructures. The principle of proposed spectrometer is based on the phonon-induced heating of the spin system of magnetic ions in semimagnetic quantum wells (QW's). In external magnetic field B, the ground electron state of the magnetic ions splits to the system of Zeeman sublevels with energy separation $\mu_B g B$. Nonequilibrium phonons with energy $\hbar\omega = \mu_B g B$ induce resonant spin-phonon transitions and as a result the population of the upper Zeeman sublevels increases, i.e., the temperature of the spin system becomes higher. Thus measuring, in some way, the spin temperature of the system as a function of a magnetic field it becomes possible to obtain the spectrum of nonequilibrium phonons, N_ω. For the first time, the idea of using the magnetic ions as a phonon spectrometer

in subterahertz region was proposed by Anderson and Sabisky[14] in 1967. They used SrF_2:Tm^{2+} single crystals and measured the population of the upper Zeeman sublevels of Tm^{2+} ions using the optical-absorption technique. Using such a phonon spectrometer, Sabisky and Anderson[15] measured the spectrum of phonon losses at the crystal surface contacted with liquid helium (He). In our recent paper, we have shown that the spin system of Mn ions in CdTe/(Cd, Mn)Te QW's may be used as a sensitive detector of ballistic nonequilibrium phonons.[16] However, it was not clear whether this phonon detection method is actually a phonon spectroscopy technique and whether the signals detected at certain magnetic field are adequate to the phonon occupation numbers N_ω with phonon energy $\hbar\omega=\mu_B g B$. Here, we present a detailed study of the heating of Mn-spin system by phonons created by heat pulse technique.[17] In the assumption that the spin system is heated by resonant phonons $\hbar\omega=\mu_B g B$ we get the phonon spectrum, which is similar to the spectrum obtained in previous experiments.[15,18] This result gives a strong argument that semimagnetic QW's are working as a phonon spectrometer and may be used in the studies of different semiconductor nanostructures (quantum wells, dots and wires, tunneling devices, superlattices).

In the present paper, we also discuss the mechanisms of spin-phonon interaction in semimagnetic QW's. This problem is strongly connected with the formation mechanism of magnetic polaron.[19,20] We discuss the interaction of acoustic phonons with magnetic clusters, the electron spectrum of which is not understood yet in details and was studied only theoretically.[21]

II. EXPERIMENTAL METHOD

The main idea of the experimental method is based on the temperature-dependent giant Zeeman effect for the exciton states in semimagnetic (Cd,Mn,Mg)Te material.[22] In the external magnetic field, the Mn ions have a system of Zeeman sublevels with energy separation $\mu_B g_{\mathrm{Mn}} B$ ($g_{\mathrm{Mn}}=2$) and at $B=7$ T, $\mu_B g_{\mathrm{Mn}} B=0.8$ meV. In our experiments, the Mn spin system is heated by nonequilibrium phonons and the spin temperature T_s is measured from the exciton photoluminescence (PL) spectrum, which has been calibrated in equilibrium conditions, i.e., without nonequilibrium phonons. The final stage is to find out whether the magnetic-field dependence $T_S(B)$ corresponds to the nonequilibrium phonon spectrum N_ω ($\hbar\omega=\mu_B g_{\mathrm{Mn}} B$), the main features of which are known from earlier studies.

We study three quantum well (QW) structures with different design in order to see whether the observed results depend on compositions of Mn or Mg and on the QW width of the semiconductor nanostructure. All of them are grown by molecular beam epitaxy on (100) semi-insulating GaAs substrates with thickness 0.3–0.4 mm. Three (Cd,Mn,Mg)Te-based heterostructures have been used in the present experiments. *Structure A* has been grown after a 350 nm-thick $Cd_{0.36}Mn_{0.07}Mg_{0.57}Te$ buffer layer. It contains five different QW's with 16-nm width separated by 32 nm-thick $Cd_{0.36}Mn_{0.07}Mg_{0.57}Te$ barriers. Materials of QW's are CdTe, $Cd_{0.93}Mn_{0.07}Te$, and $Cd_{0.93-y}Mn_{0.07}Mg_yTe$ digital alloys ($y=0.25$, 0.50, 0.75), where y an efficient Mg concentration. The digital alloys are in fact

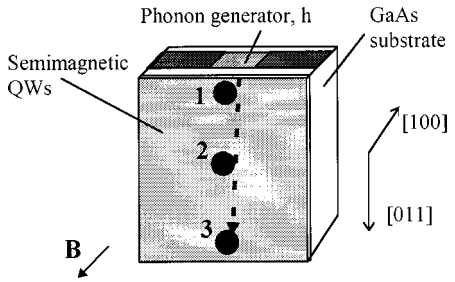

FIG. 1. The experimental setup. Black spots (points 1, 2, and 3) on the surface with QW's show the places where excitons were excited. The dashed arrow shows ballistic phonons traveling from *h* to point 3. Corresponding distances (in mm) between *h*, and points 1, 2, and 3 are $r=0.3$, 1.5, 2.5.

$Cd_{0.93}Mn_{0.07}Te/Cd_{0.36}Mn_{0.07}Mg_{0.57}Te$ short-period superlattices (25 periods). Respective layer thickness are 0.48 nm/0.16 nm for $y=0.25$, 0.32 nm/0.32 nm for $y=0.50$, and 0.16 nm/0.48 nm for $y=0.75$ (for details see Ref. 23). *Structure B* has been grown after a 480 nm-thick $Cd_{0.64}Mn_{0.06}Mg_{0.3}Te$ buffer layer. The Mn concentration of 0.06 was kept constant through the structure, which contains eight identical parabolic QW's of 18-nm width separated by 25 nm-thick $Cd_{0.64}Mn_{0.06}Mg_{0.3}Te$ barriers. The parabolic profile was formed by the modulation of the Mg component concentration, which equals to zero in the center of the QW (for details see Ref. 24). *Structure C* is $CdTe/Cd_{0.6}Mn_{0.4}Te$ QW's heterostructure. The structure contains four CdTe QW's with different widths (9.0, 4.0, 1.8, and 1.2 nm). The QW's are separated by 50 nm-thick $Cd_{0.6}Mn_{0.4}Te$ barriers (for details see Ref. 25). The wafers were cut to pieces with the area 3×4 mm^2 of the surface with QW's.

The experimental setup is shown in Fig. 1. We generate nonequilibrium phonons using the well-known heat pulse technique.[17] The phonon generator, *h* (10-nm constantan film), with an area 0.5×0.25 mm^2 was evaporated on the narrow side of the GaAs substrate and was heated by current pulses with duration 0.15 μs, pulse-power density up to $P=400$ W/mm^2 and repetition rate of 20 kHz. The phonons generated in *h* during the current pulse have a Planck distribution, characterized by a heater temperature $T_h \propto P^{1/4}$. The value of T_h may be calculated from the acoustic mismatch theory.[26] Then, nonequilibrium phonons with a broad spectrum having characteristic energies of about several meV (i.e., $10^{11}-10^{12}$ Hz) are injected into the GaAs substrate. The phonons propagating in the GaAs reach the semimagnetic QW structure and induce changes in the exciton luminescence, which is excited by *cw* Ar laser (excitation power 5 mW, the diameter of the focused spot on the sample 0.3 mm) in a certain point at the surface of QW's (i.e., point 1, 2, or 3, Fig. 1). The exciton photoluminescence (PL) from the QW's is focused on an input slit of a 1-m spectrometer, detected by a fast photomultiplier and finally analyzed with the time resolution up to 10 ns by means of a special interface board and a computer. The sample is mounted inside a superconducting magnet in the Faraday configuration and is immersed in pumped liquid helium, $T_0=1.6$ K.

The existence of paramagnetic Mn ions in the structures leads to the giant Zeeman splitting of an exciton line in the presence of magnetic field *B*. This phenomenon is well

known to be due to the strong interaction between carriers and paramagnetic Mn ions.[22,27] Experimentally the splitting of exciton states may be displayed as a redshift ΔE of the exciton PL line at low temperatures. From the earlier studies the value of ΔE is known to decrease rapidly with increasing temperature.[22] The reason for that is the decrease of magnetization, when the orientation of Mn spins in external field decreases due to the thermal occupation of higher Zeeman sublevels of Mn ions. In the present experiments we explore the nonequilibrium phonons generated by a heat pulse in order to elevate the temperature of Mn-ions system T_S and, thus, to decrease the exciton Zeeman splitting. In a recent work of Kulakovskii *et al.*[28] the heating of Mn spins was induced by the hot electron plasma at high-optical excitation density. In our present experiments, we use low-optical excitation density and the dynamical shift of the exciton line $\delta E(t)$ (i.e., variation of ΔE during the heat pulse), is induced only by nonequilibrium phonons. We measure the spin-heating effect in three points located at different distances r from the phonon generator (points 1, 2, and 3 see Fig.1). The different heater temperatures T_h and magnetic fields up to 7 T are used. As a result, we obtain magnetic-field dependence of the spin temperature T_S of Mn ions in the presence of nonequilibrium phonons in different samples and QW's.

As an example, we describe the procedure of obtaining T_S in the presence of nonequilibrium phonons for sample B at $B=3.0$ T. The exciton PL lines are shown in Fig. 2(a). They correspond to the annihilation of exciton at the lower energy state. The energy position of exciton luminescence line depends strongly on the magnetic field B and the bath temperature T_0. Curve 1 corresponds to the spectrum measured at $T_0=1.6$ K and $B=0$. The low-energy shift $\Delta E=28$ meV of the exciton line is observed at $B=3$ T [curve 2, Fig. 2(a)]. This shift decreases at elevated temperature (curve 3, $T_0=4.2$ K, $B=3$ T). In our example [Fig. 2(a)] it is important that the shape and the intensity of the exciton line does not change significantly while T_0 is elevated (compare curves 2 and 3). The shift ΔE may be described by the well-known equation[22]

$$\Delta E=\gamma B_{5/2}\left[\frac{5\mu_B g_{\mathrm{Mn}} B}{2k_B(T_S+T_1)}\right], \tag{1}$$

where $B_{5/2}(z)$ is Brillouin function, γ and T_1 are depending on Mn-concentration efficient parameters. In Eq. (1) the magnetic polaron effects are not included, which in our samples is valid for $B>1.5$ T, where the contribution of magnetic polarons is suppressed.[29,30]

The dashed curve in Fig. 2(a) shows the spectrum measured in the presence of nonequilibrium phonons ($T_h=20$ K) in the detection point 1 at $T_0=1.6$ K and $B=3$ T in the ''time window'' ($\Delta t=0.6\,\mu$s) at the time corresponding to the maximum changes during the phonon pulse [see dashed area in Fig. 2(b)]. It is seen that the dashed curve is shifted to the higher energies in respect to curve 2 measured at the same B in the absence of nonequilibrium phonons. The spectral shape of the dashed curve and curve 2 are almost identical and the observed amplitude of the time-dependent shift, $\delta E(t)$, measured at the high-energy wing of exciton luminescence line is equal to 3 meV and corresponds to the heating of spin system of Mn ions by nonequilibrium phonons.

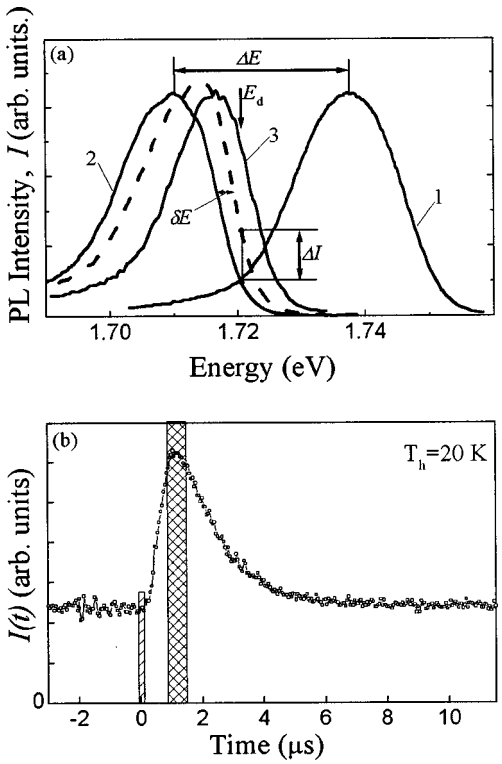

FIG. 2. (a) Luminescence spectra of sample B measured in equilibrium conditions (solid lines) at $T_0=1.6$ K (curve 1, $B=0$ T; curve 2, $B=3$ T) and $T_0=4.2$ K (curve 3, $B=3$ T). Dashed line shows the spectrum measured in the presence of nonequilibrium phonons in point 1 ($T_h=20$ K, $B=3$ T) in the ''time window'' corresponding to the maximum changes during the phonon pulse [shown by shaded area in (b)]. (b) Phonon induced luminescence pulse measured in point 1 ($T_h=20$ K, $B=3$ T) at the photon energy $E_d=1.721$ eV [shown by vertical arrow in (a)]. The dashed area shows a current pulse.

For the most values of B and T_h used in our experiments we can obtain the dynamical shift $\delta E(t)$ by measuring phonon induced luminescence pulse $I(t)$ [Fig. 2(b)] at the fixed energy E_d [shown by an arrow in Fig. 2(a)], which corresponds to the high-energy edge of the exciton line. Thus, comparing the relative increase of the luminescence intensity $\Delta I(t)/I_0$ [here, $\Delta I(t)=I(t)-I_0$, I_0 is the stationary intensity without nonequilibrium phonons, $T_0=1.6$ K] with the shape of the exciton line [in our example curve 2 in Fig. 2(a)] we may obtain the dynamical shift $\delta E(t)$ at any delay time t_d. This is realized by the parallel shift of equilibrium spectrum [curve 2 in Fig. 2(a)] until the intensity at E_d will be equal to corresponding intensity $I(t')$. In our example, such procedure gives $\delta E=3$ meV for t_d corresponding to the maximum of $\Delta I(t)$, which is equal to the value obtained with ''time-window'' technique. Further, in the next section, where we describe the experimental results, we shall consider only the case of relatively small δE, so that $\Delta I(t) \propto \delta E(t)$.

The next step is to determine the spin temperature T_S in the presence of nonequilibrium phonons from the measured δE using the obvious fact that in equilibrium $T_S=T_0$. In

TABLE I. Experimentally obtained values of γ and T_1 for samples *A*, *B*, and *C*.

Sample		γ (meV)	T_1 (K)
A	$y=0.25$	40.4	2.9
	$y=0.50$	36.6	3.4
B		39.6	3.2
C		13.8	2.4

most cases it is possible to use Eq. (1) with parameters γ and T_1 determined from the equilibrium dependencies of ΔE or δE on B and T_0. Parameters γ and T_1 are presented in the Table I and curves in Fig. 3 show the calculated dependencies T_S as a function of δE for different B in sample *B*. The dependencies of $T_S(\delta E)$ were measured experimentally in equilibrium conditions ($T_S=T_0$) for the different values of B and T_0 (see symbols in Fig. 3).

The described procedure of getting the values of T_S and δE is not exactly valid for high density of phonons in the detection point and correspondingly high T_S. In this case, nonequilibrium phonons additionally induce the changes in the shape of the exciton luminescence line and the resulting δE cannot be obtained accurately. The changing of the shape of the exciton line in the presence of nonequilibrium phonons with high density ($T_h=40$ K, point 1) is shown in Fig. 4. The different curves in Fig. 4 are the spectra measured in ''time windows'' with different delays t_d after phonon pulses. The spectrum measured at $t_d=10.65\,\mu$s (curve 4) is identical with the equilibrium spectrum ($T_0=1.6$ K). Similar changes of the shape of the luminescence line induced by nonequilibrium phonons with high density are also observed in zero-magnetic field. The reason of changing in the shape of the exciton PI line in the presence of nonequilibrium phonons is not clear and the understanding of this unusual behavior requires more experimental work. Apparently this is connected with the effect of nonequilibrium phonons on the system of photoexcited carriers and excitons. It may be so that nonequilibrium phonons have different effects on the excitons with different energies, which form the inhomogeneously broadened shape of the exciton PL line.

Thus, measuring the dynamical shift δE of the exciton line in the presence of nonequilibrium phonons with low density we may obtain the temperature T_S of the Mn-spin system.

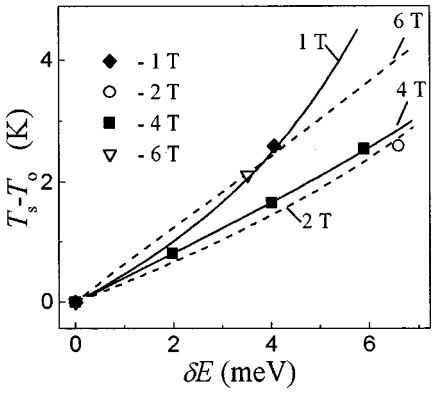

FIG. 3. The calculated (lines) and measured (symbols) changes of spin temperature T_S-T_0 as a function of the shift δE for different magnetic fields in sample *B* ($T_0=1.6$ K).

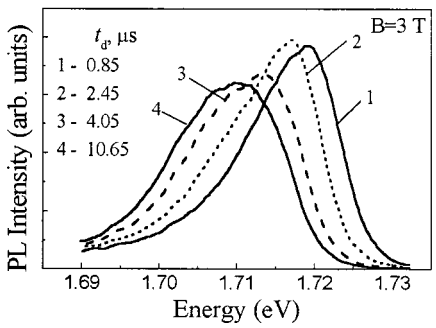

FIG. 4. Luminescence spectra in the presence of nonequilibrium phonons with high density (sample *B*, $T_h=40$ K, point 1) measured in ''time windows'' $\Delta t=0.6\,\mu$s at different time delays t_d.

III. EXPERIMENTAL RESULTS

In the experiments, we studied the phonon-induced effect on the exciton PL in different samples and QW's, detection points, at different magnetic fields B and heater temperatures T_h. The main experimental results concern the temporal evolution of the phonon-induced signals $\Delta I(t)$ and the dependencies of T_S on B. These results do not differ qualitatively for different samples, QW's and detection points. The observed dependencies of T_S on B are very similar in a wide range of T_h. Thus, we limit the presentation of the experimental results by some typical examples of signals $\Delta I(t)$ and dependencies $T_S(B)$, when $T_S<5$ K. For a higher value of T_S nonlinear effects (see Sec. II) and overheating problems cause experimental difficulties in accurate determination of T_S.

Figure 5 shows normalized phonon-induced signals $\Delta I(t)\propto\delta E(t)$ for different B measured at different detection points and in different samples. In all experiments, $\Delta I(t)$ have a sharp rising edge the duration of which does not depend on B [Fig. 5(a)]. The duration of the rising edge increases while the distance r between the heater h and the detection point increases [Fig. 5(b)]. The horizontal bars in Fig. 5(b) show the expected delay of $\Delta I(t)$ measured in point 1 and 2 with the increase of the distance r if propagation of phonons in GaAs is ballistic (e.g., without scattering) on the path from the heater to the detection point 1 and 2 correspondingly (delay$=r_2-r_1/v_j$, v_j—sound velocity of phonon with j polarization). It is seen that there is a good agreement between the observed delay of the leading edges and the expected ''ballistic delays.'' The duration of the trailing edges of $\Delta I(t)$ have a value of several microseconds. This value depends slightly on B [see Fig. 5(a)] and is almost independent of the distance from the heater to the detection point [see Fig. 5(b)]. Figure 5(c) shows $\Delta I(t)$ measured for the same B, T_h, and r but in different samples that have different designs and Mn and Mg contents. It is seen that the temporal shapes $\Delta I(t)$ are almost identical and, as it was mentioned earlier, $\Delta I(t)$ does not strongly depend on the sample.

Figure 6 shows the examples of the magnetic-field dependencies of T_S at the time corresponding to the maximum of $\Delta I(t)$ measured for different samples and QW's. The remarkable fact is that T_S is not constant with changing of B and we see the *decrease of* T_S *with the increasing of magnetic field*. This behavior is qualitatively the same in all

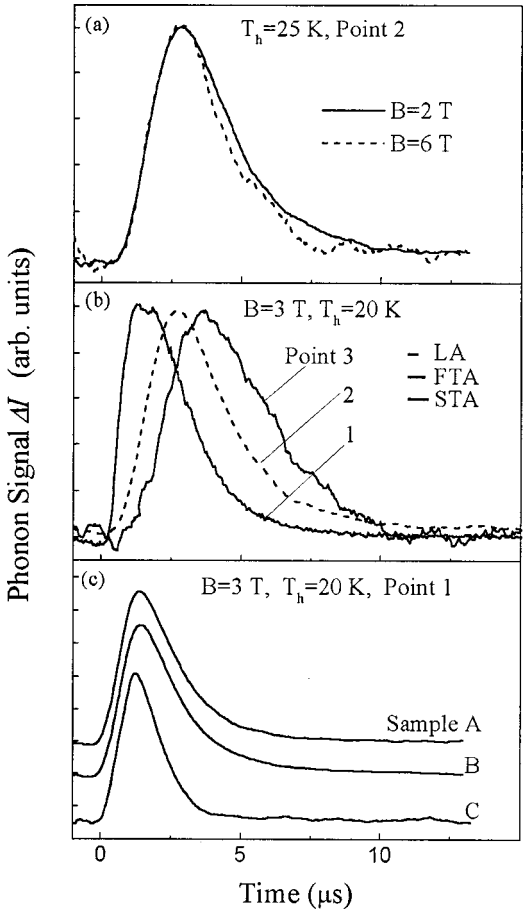

FIG. 5. The temporal evolution of the phonon induced PL signals, $\Delta I(t)$, (normalized, linear scale), measured in different magnetic fields (a), detection points (b), and samples (c). Horizontal bars in (b) show the expected ballistic time shifts between phonon signals measured in points 1 and 2 for LA, FTA, and STA phonons with velocities 5.3, 3.4, and 2.5 km/s, respectively. Panels (a) and (b) correspond to sample *B*.

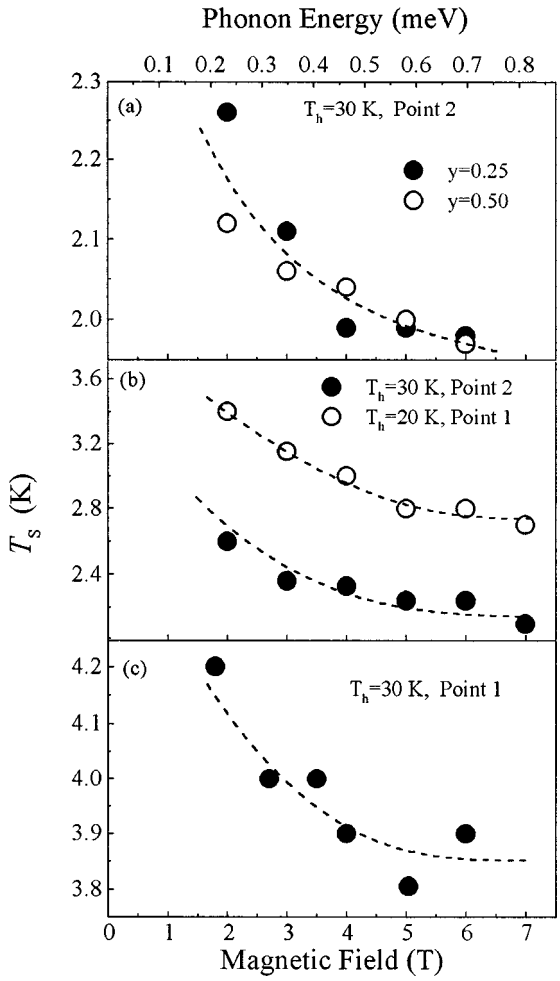

FIG. 6. Spin temperature T_S as a function of magnetic field (lower scale) and phonon energy (upper scale) for samples *A* (a), *B* (b), and *C* (c). Dashed lines are guides to the eye.

samples and QW's. The decrease of $T_S(B)$ with B is observed in a wide range of $T_h = 20-40$ K and in different detection points.

IV. DISCUSSION

The main idea of the analysis is to show that assuming that the spin heating is induced by resonant phonons $\hbar\omega = \mu_B g_{\mathrm{Mn}} B$, we are able to get the known phonon spectrum N_ω from the measured dependence $T_S(B)$. If we will obtain that $T_S(B)$ corresponds to the known N_ω ($\hbar\omega = \mu_B g_{\mathrm{Mn}} B$) then we may conclude that spin-heating effect is actually induced by resonant phonons and the technique is working as a phonon spectrometer. On the first stage of the discussion, we will analyze the temporal evolution of the measured signals $\Delta I(t)$. We will show that the spin heating is induced by ballistic phonons. Thus, we obtain roughly the range of phonon energies (<1 meV) which are active in the spin-heating effect. On the next stage, we will discuss the main features of the nonequilibrium phonon spectrum in the detection point. On the final stage, we will compare field dependencies $T_S(B)$ with the qualitatively known N_ω assuming that $\hbar\omega = \mu_B g_{\mathrm{Mn}} B$ and will make a conclusion about the main role of the resonant phonons in the spin-heating effect.

The signals $\Delta I(t)$ (Fig. 5) are governed by the time evolution of phonon occupation numbers $N_\omega(t)$ and the time response of our phonon detection technique. The response time of our phonon detection technique has two contributions. The first is related to the lifetime of excitons, which is known to be very short [~0.2 ns (Ref. 31)] in comparison with the duration of the measured signals $\Delta I(t)$. The second contribution is related to the response time of the spin system τ_S. This time is equal to the spin-lattice relaxation time, which depends on Mn concentration and magnetic-field value.[32] The mechanism of spin-lattice relaxation in semimagnetic semiconductors like (Cd,Mn,Mg)Te is not understood in detail yet. Experimental data for $Cd_{1-x}Mn_xTe$ $x = 0.06-0.07$ gives $\tau_S \sim 0.1\ \mu$s.[32] Thus, the relaxation time τ_S in principle, may slightly influence the rising edges of $\Delta I(t)$, which has duration of 0.5 μs, but the value of $\tau_S \sim 0.1\ \mu$s is much shorter than the average duration of all measured signals $\Delta I(t)$ (Fig. 5). Therefore, we may consider that the spin system is in quasiequilibrium with nonequilibrium phonons and $\Delta I(t)$ reflects the time evolution of phonon occupation numbers $N_\omega(t)$ rather than the spin-lattice relaxation process.[33] This means that if the spin system is heated by resonant phonons $\hbar\omega = \mu_B g_{\mathrm{Mn}} B$ the balance between spin-

phonon transitions with emission and absorption of phonons gives

$$\exp\left[-\frac{\mu_B g_{\mathrm{Mn}} B}{k_B T_S}\right]=\frac{N_\omega}{N_\omega+1}. \tag{2}$$

It is well known that low-energy phonons with $\hbar\omega<1$ meV travel ballistically for distances of few mm, while high-energy phonons $\hbar\omega\gg1$ meV are strongly scattered (scattering rate is proportional to ω^4) by isotopes and impurities and thus travel diffusive.[1,2,17,34] The exact value of the energy boundary between ballistics and diffusion depends on the distance from a heater and on the sample quality and thus cannot be obtained accurately in our experiments. The corresponding mean-free path of high-energy phonons in high-quality, undoped GaAs samples has a value of $l=1.8$ mm for $\hbar\omega=2$ meV.[34] Our GaAs samples are commercial, semi-insulating substrates prepared for MBE growth. It is known that phonons with $\hbar\omega>1$ meV are effectively scattered in such samples and we cannot expect for these phonons l to be higher than 1 mm.[35,36] The time evolution of the detected phonon signal enables to say whether the phonon propagation is ballistic or diffusive. If the rising edge of the signal is sharp (~0.1 μs) and the delay corresponds to ballistic time, the signal is induced by ballistic, low-energy phonons. If the time evolution shows long ($\gg1$ μs) rising and trailing edge, the amplitude of the signal rapidly decreases and the shape broadens with the increase of r, then the propagation is mainly diffusive, which means that high-energy phonons are detected. The examples of ballistic and diffusive phonon signals may be found elsewhere.[1,2,17,34] The measured $\Delta I(t)$ (Fig. 5) and correspondingly $N_\omega(t)$ is that the observed propagation of phonons from the heater to the detection point is mainly *ballistic*. Actually, the increase of the distance r does not change essentially the trailing edges of $\Delta I(t)$ and only the *delay corresponding to the ballistic times is observed* [Fig. 5(b)]. The increase of the duration of the leading edge of $\Delta I(t)$ with increase of r is obviously due to the different sound velocities v_j of phonons with different modes (LA, FTA, STA). However, we cannot accurately resolve different phonon modes and the total duration of $\Delta I(t)$ is rather long in comparison with standard ballistic phonon experiments.[17] Partly this is due to relative effects of the heater h and detector sizes (0.5×0.2 mm^2 and 0.2 mm diameter correspondingly). This should smear $\Delta I(t)$ in time for 0.2 μs. But the main reason of long (up to 5 μs) $\Delta I(t)$ we see in the specific geometry of our experiments (Fig. 1) when phonons are propagating in a thin (<0.4 mm) GaAs sample and the contribution to $\Delta I(t)$ from the phonons reflected at the surface on the way from h to the detection point becomes essential.[37,38] Thus, from the delay of the leading edges of $\Delta I(t)$ with the increase of r, we conclude that the observed signals $\Delta I(t)$ are induced by ballistic phonons. That means that our phonon detection technique is sensitive to low-energy ($\hbar\omega<1$ meV) phonons.

Now we turn to the discussion of nonequilibrium phonon spectrum in the detection point. Experimental results (Fig. 6) clearly show that phonon system is actually nonequilibrium and cannot be described by a Bose-Einstein distribution with a certain temperature. Indeed, if thermalization of phonons takes place, the spin temperature T_S would be independent on the magnetic field. Experiments (Fig. 6) show the decrease of T_S with B. Thus, we exclude phonon thermalization in the detection point. Then nonequilibrium phonon spectrum N_ω may be described as a distribution with energy-dependent effective temperature

$$N_\omega=\{\exp[-\hbar\omega/k_B T_{\mathrm{eff}}(\omega)]-1\}^{-1}. \tag{3}$$

In equilibrium, the phonon spectrum is Planckian and correspondingly T_{eff} does not depend on ω. In the detection point, the phonon spectrum is nonequilibrium and $T_{\mathrm{eff}}(\omega)$ is not constant with ω. In Eq. (3) N_ω includes both ballistic phonons from the heater h, which reach the detector and equilibrium bath phonons with $T_0=1.6$ K. In our experimental geometry (Fig. 1) the important factor contributing to N_ω is the dependence of phonon losses at sample surface contacted with liquid He. This dependence is well known to be almost universal for all solids and determined by great acoustic mismatch in the solid and liquid He for low-energy phonons and Kapitza anomaly for high-energy phonons.[15,18,39] *The losses of phonons from the sample to liquid He increases with the phonon energy*. The transition energy region between phonons completely reflected from the surface and the phonons which are $\sim$50% transmitted to liquid He corresponds to ≈0.4 meV (0.1 THz).[15,18] Thus, in the detection point $T_{\mathrm{eff}}(\omega)$ ($\hbar\omega=0.3$–0.5 meV) should decrease with the increase of ω. As we have shown the spin system is in equilibrium with nonequilibrium phonons and if the spin heating is induced by resonant phonons $\hbar\omega=\mu_B g_{\mathrm{Mn}} B$ from Eqs. (2) and (3) we get that

$$T_S(B)=T_{\mathrm{eff}}(\omega). \tag{4}$$

Thus, the decrease of $T_{\mathrm{eff}}(\omega)$ with ω should lead to the decrease of T_S with B.

Experimentally, we actually observe (Fig. 6) that T_S decreases with the increase of B. The upper scale of Fig. 6 shows the phonon energies $\hbar\omega=\mu_B g_{\mathrm{Mn}} B$. The energy range corresponds to the same frequency range studied in the previous experiments where the phonon-energy dependence of phonon losses to liquid He has been established.[15,18] Thus, we get that the measured field dependence of T_S reflects the nonequilibrium phonon spectrum. The qualitative agreement of the observed dependence $T_S(B)$ with the corresponding phonon spectrum leads us to the conclusion that our main assumption that the spin-heating effect is induced by resonant phonons $\hbar\omega=\mu_B g_{\mathrm{Mn}} B$ (direct spin-phonon transitions) becomes true and *the technique is working as a phonon spectrometer*.

In our experimental geometry (Fig. 1), phonon losses at solid/liquid He boundary should influence the decay of $\Delta I(t)$, which is governed mainly by the phonons reflected from the sample surface. Qualitatively we see that the decay of $\Delta I(t)$ at low B is slightly longer than at high B [compare solid and dashed curves in Fig. 5(a)]. Such experimental observation confirms the conclusion about actually measuring the phonon spectrum, which is determined by energy dependence of phonon losses to liquid He.

The magnetic-field dependencies $T_S(B)$ are qualitatively the same for all studied samples and QW's. The decrease of T_S with B is observed in different detection points and in a wide range of $T_h=20$–40 K. Such universal behavior also

confirms the statement about measuring the phonon spectrum because the energy dependence of phonon losses to liquid He should not depend strongly on the design of the structure and density of phonons in the detection point.

Let us discuss another possible explanation of experimental results taking into account the role of spin-phonon transitions in antiferromagnetic clusters of Mn ions. The clusters of Mn ions are known to be formed at high-Mn concentration ($x>0.01$).[40] From the theory it is known that clusters of Mn ions have the first excited state with the energy of several meV and this energy decreases with magnetic field.[21] Then the spin system may be heated not only by the *direct* process induced by resonant phonons $\hbar\omega=\mu_B g B<1$ meV but also by high-energy phonons $\hbar\omega>1$ meV that are resonant with the excited state (*indirect* Orbach process). In this case, the dependence of T_S on magnetic field (Fig. 6) may be attributed to the dependence of the spectrum of the excited states on B. Also the dependence $T_S(B)$ may be explained by the B dependence of relative contribution of direct and indirect transitions.[16] However, the explanation of the experimental results by the indirect spin-phonon transitions seems to us not reasonable. The main argument against indirect model is that such transitions require much higher phonon energies than $\hbar\omega=\mu_B g_{\mathrm{Mn}} B$. Even, if phonons ($\hbar\omega>1$ meV) would reach the detection points 2 and 3 and give contribution to the heating of spin system, the time evolution of $\Delta I(t)$ measured in these points should be very different from $\Delta I(t)$ measured in point 1. In the present experiments, we do not see the strong dependence of $\Delta I(t)$ either on the detection point or on the magnetic field (Fig. 5). Thus, we conclude that the contribution from the high-energy phonons and correspondingly indirect spin-phonon transitions are not important for the experimentally observed heating effect of the Mn-spin system. However, we do not exclude completely the role of indirect Orbach and Raman processes. They may result in some constant background in the dependencies of $T_S(B)$, which causes difficulties in obtaining quantitative values of T_{eff}. The indirect processes may become very important for higher phonon densities and correspondingly higher T_S.

V. CONCLUSIONS

Finally, we study the heating of spin system of magnetic ions in semimagnetic quantum wells by acoustic nonequilibrium phonons. The optical method of registration based on the giant Zeeman effect of exciton states has been exploited. We find that the heating of the spin system is induced by ballistic, subterahertz phonons, and the spin temperature decreases with the magnetic field increase. The results may be consistently explained in the model suggesting the heating of the spin system by resonant phonons with $\hbar\omega=\mu_B g_{\mathrm{Mn}} B$. The known spectrum of nonequilibrium phonons in quantum wells, which is determined by the phonon losses at solid/liquid He boundary has been detected for all measured samples.

The technique of the exciton luminescence detection of nonequilibrium phonons combined with semimagnetic semiconductor quantum wells may be used as a *phonon spectrometer* in semiconductor nanostructures. The resolution of such spectrometer should be very fine and limited by the width of the Zeeman sublevels. For moderate Mn concentration ($x<0.1$) this value is about 0.01 meV and is determined by the processes of spin-spin interaction.[41] Presence of the magnetic ion system is the principle requirement for the suggested phonon spectrometer. Therefore, it can be realized on the base of II-VI semimagnetic semiconductor materials [(Cd,Mn)Te, (Zn,Mn)Se, etc.] which magnetic and optical properties and technological aspects are known very well (for review see Ref. 40). Very recently a great progress has been reported for the III-V semiconductor material doped with magnetic ions, namely (Ga,Mn)As.[42] One can also think about creation of hybrid structures, when the II-VI semimagnetic materials are overgrown on III-V semiconductor heterostructure. We point out here that structures studied in the present paper were grown of GaAs substrates.

ACKNOWLEDGMENTS

We acknowledge I. A. Merkulov, A. A. Kaplyanskii, and V. P. Kochereshko for helpful discussions and D. A. Mazurenko for technical support. This work has been supported by the NATO (Grant No. CRC 971360), Volkswagen Foundation, Russian Foundation for Fundamental Research (Grant No. 99-02-18276), Russian Ministry of Science (Grant No. 99-3011), and Polish State Committee for Scientific Research (Grant No. PBZ 028 11/P8).

*Also at A. F. Ioffe Physical-Technical Institute, St. Petersburg, Russia.

[1] *Nonequilibrium Phonon Dynamics*, Vol. 124 of *NATO Advanced Study Institute, Series B: Physics*, edited by W. E. Bron (Plenum, New York, 1985).

[2] *Nonequilibrium Phonons in Nonmetalic Crystals*, edited by W. Eisenmenger and A. A. Kaplyanskii, Modern Problems in Condensed Matter Sciences Vol. 16 (North-Holland, Amsterdam, 1986).

[3] L. J. Challis and A. J. Kent, in *Die Kunst of Phonons, Lectures from the XXIX Winter School of Theoretical Physics*, edited by T. Pazkewicz and K. Rapcewicz (Plenum, New York, 1994), p. 159.

[4] A. V. Akimov, E. S. Moskalenko, L. J. Challis, and A. A. Kaplyanskii, Physica B **219&220**, 9 (1996).

[5] W. Eisenmenger, in *Physical Acoustics*, edited by W. P. Mason and R. N. Thurston (Academic, New York, 1976), Vol. 12, p. 79.

[6] V. Narayanamurti, H. L. Stormer, M. A. Chin, A. C. Gossard, and W. Wiegmann, Phys. Rev. Lett. **43**, 2012 (1979).

[7] S. Tamura, D. C. Hurley, and J. P. Wolfe, Phys. Rev. B **38**, 1427 (1988).

[8] J. C. Hensel, P. I. Halperin, and R. C. Dynes, Phys. Rev. Lett. **51**, 2302 (1983).

[9] M. Rothenfusser, J. Kösfer, and W. Dietsche, Phys. Rev. B **34**, 5518 (1986).

[10] M. T. Ramsbey, I. Szafarek, G. Stillman, and J. P. Wolfe, Phys. Rev. B **49**, 16 427 (1994).

[11] E. S. Moskalenko, A. L. Zhmodikov, A. V. Akimov, A. A. Kaplyanskii, L. J. Challis, T. C. Cheng, and O. H. Hughes, Ann. Phys. (Leipzig) **4**, 127 (1996).
[12] F. F. Ouali, N. N. Zinov'ev, L. J. Challis, F. W. Sheard, M. Henini, D. P. Stenson, and K. P. Strickland, Phys. Rev. Lett. **75**, 308 (1995); S. A. Cavill, A. V. Akimov, F. F. Ouali, L. J. Challis, A. J. Kent, and M. Henini, Physica B **263-264**, 537 (1999).
[13] J. Cooper, S. Roshko, W. Dietsche, and Y. Kershaw, Phys. Rev. B **50**, 8352 (1994).
[14] C. H. Anderson and E. S. Sabisky, Phys. Rev. Lett. **18**, 236 (1967).
[15] E. S. Sabisky and C. H. Anderson, Solid State Commun. **17**, 1095 (1975).
[16] A. V. Akimov, A. V. Scherbakov, A. L. Zhmodikov, V. P. Kochereshko, D. R. Yakovlev, W. Ossau, G. Landwehr, T. Wojtowicz, G. Karczewski, and J. Kossut, Phys. Rev. B **56**, 12 100 (1997).
[17] R. J. von Gutfeld, in *Physical Acoustics*, edited by W. P. Mason (Academic, New York, 1958), Vol. 5, p. 233.
[18] O. Koblinger, E. Dittrich, U. Heim, M. Welte, and W. Eisenmenger, in *Phonon Scattering in Condensed Matter*, edited by W. Eisenmenger, K. Lassman, and S. Döttinger (Springer-Verlag, Berlin, 1984), pp. 209–211.
[19] T. Dietl, P. Peyla, W. Grishaber, and Y. Merle d'Aubigne, Phys. Rev. Lett. **74**, 474 (1995).
[20] D. R. Yakovlev and K. V. Kavokin, Comments Condens. Matter Phys. **18**, 51 (1996).
[21] D. Scalbert, Phys. Status Solidi B **193**, 189 (1996).
[22] J. A. Gaj, R. Planel, and G. Fishman, Solid State Commun. **29**, 435 (1979).
[23] M. Kutrowski, G. Karczewski, G. Cywinski, M. Surma, K. Grasza, E. Lusakowska, J. Kossut, T. Wojtowicz, R. Fiederling, D. R. Yakovlev, G. Mackh, U. Zender, and W. Ossau, Thin Solid Films **306**, 283 (1997).
[24] T. Wojtowicz, G. Karczewski, and J. Kossut, Thin Solid Films **306**, 279 (1997).
[25] G. Mackh, W. Ossau, D. R. Yakovlev, G. Landwehr, R. Hellman, E. O. Göbel, T. Wojtowicz, G. Karczewski, and J. Kossut, Solid State Commun. **96**, 297 (1995).
[26] W. Kappus and O. Weiss, J. Appl. Phys. **44**, 1947 (1973).
[27] B. Kuhn-Henrich, M. Popp, W. Ossau, E. Bangert, A. Waag, and G. Landwehr, Semicond. Sci. Technol. **8**, 1239 (1993).
[28] V. D. Kulakovskii, M. G. Tyazhlov, A. I. Filin, D. R. Yakovlev, A. Waag, and G. Landwehr, Phys. Rev. B **54**, R8333 (1996).
[29] D. R. Yakovlev, K. V. Kavokin, I. A. Merkulov, G. Mackh, W. Ossau, R. Hellman, E. O. Göbel, A. Waag, and G. Landwehr, Phys. Rev. B **56**, 9782 (1997).
[30] D. R. Yakovlev, W. Ossau, G. Landwehr, R. N. Bicknell-Tassius, A. Waag, K. V. Kavokin, A. V. Kavokin, I. N. Uraltsev, and A. Pohlman, *Proceedings of the 21st International Conference on the Physics of Semiconductors, Beijing, China, 1992* (World Scientific, Singapore, 1992), p. 1136.
[31] E. O. Göbel, R. Hellmann, G. Mackh, D. R. Yakovlev, W. Ossau, A. Waag, and G. Landwehr, Mater. Sci. Forum **182-184**, 519 (1995).
[32] T. Strutz, A. M. Mitowski, and P. Wyder, Phys. Rev. Lett. **68**, 3912 (1992).
[33] In order to check that τ_s, in principle, influences the shape of $\Delta I(t)$ we carried out similar experiments on the samples with low-Mn content ($x=0.016$, 0.025, and 0.032) and revealed a strong increase of the duration (up to 30 μs for $x=0.016$ and $B=2$ T) of $\Delta I(t)$ with the decrease of x and B. The time evolution of $\Delta I(t)$ in this case was obviously governed by the spin-lattice relaxation time, in contrast to the experiments described in the present paper.
[34] M. T. Ramsbey, S. Tamura, and J. P. Wolfe, Phys. Rev. B **46**, 1358 (1992).
[35] Z. Xin, F. F. Ouali, L. J. Challis, B. Salce, and T. C. Cheng, Physica B **219&220**, 56 (1996).
[36] A. V. Akimov, A. A. Kaplyanskii, M. A. Pogarskii, and V. K. Tihomirov, Pis'ma Zh. Eksp. Teor. Fiz. **43**, 205 (1986) [JETP Lett. **43**, 259 (1986)].
[37] S. A. Basun, S. P. Feofilov, A. A. Kaplyanskii, and W. M. Yen, Phys. Rev. Lett. **67**, 3110 (1991).
[38] In our recent preliminary experiments (unpublished) in thick (2 mm) GaAs substrates and the heater *h* opposite to the layer with QW's, we observe signals $\Delta I(t)$, which are much shorter than in the present work. This also confirms that relatively long duration of signals $\Delta I(t)$ (Fig. 5) is connected with the specific geometry of the experiments.
[39] I. M. Khalatnikov, Zh. Eksp. Teor. Fiz. **22**, 687 (1952).
[40] J. K. Furdyna, J. Appl. Phys. **64**, R29 (1988), and references therein.
[41] R. E. Kremer and J. K. Furdyna, Phys. Rev. B **32**, 5591 (1985).
[42] H. Ohno, A. Shen, F. Matsukura, A. Oiwa, A. Endo, S. Katsumoto, and Y. Iye, Appl. Phys. Lett. **69**, 363 (1996).